MOLECULAR AND CELLULAR BIOLOGY, June 2006, p. 4074–4085 Vol. 26, No. 11
0270-7306/06/$08.00+0 doi:10.1128/MCB.00095-06

Genesis of and Trafficking to the Maurer's Clefts of *Plasmodium falciparum*-Infected Erythrocytes†

Cornelia Spycher,[1] Melanie Rug,[2] Nectarios Klonis,[3] David J. P. Ferguson,[4] Alan F. Cowman,[2] Hans-Peter Beck,[1] and Leann Tilley[3]*

Department of Medical Parasitology and Infection Biology, Swiss Tropical Institute, Socinstrasse 57, CH 4002 Basel, Switzerland[1]; The Walter and Eliza Hall Institute of Medical Research, 1G Royal Parade, Parkville, Melbourne 3050,[2] and Department of Biochemistry and ARC Centre of Excellence for Coherent X-Ray Science, La Trobe University, Melbourne 3086,[3] Victoria, Australia; and Nuffield Department of Pathology, John Radcliffe Hospital, Oxford OX3 9DU, United Kingdom[4]

Received 16 January 2006/Returned for modification 15 February 2006/Accepted 4 March 2006

Malaria parasites export proteins beyond their own plasma membrane to locations in the red blood cells in which they reside. Maurer's clefts are parasite-derived structures within the host cell cytoplasm that are thought to function as a sorting compartment between the parasite and the erythrocyte membrane. However, the genesis of this compartment and the signals directing proteins to the Maurer's clefts are not known. We have generated *Plasmodium falciparum*-infected erythrocytes expressing green fluorescent protein (GFP) chimeras of a Maurer's cleft resident protein, the membrane-associated histidine-rich protein 1 (MAHRP1). Chimeras of full-length MAHRP1 or fragments containing part of the N-terminal domain and the transmembrane domain are successfully delivered to Maurer's clefts. Other fragments remain trapped within the parasite. Fluorescence photobleaching and time-lapse imaging techniques indicate that MAHRP1-GFP is initially trafficked to isolated subdomains in the parasitophorous vacuole membrane that appear to represent nascent Maurer's clefts. The data suggest that the Maurer's clefts bud from the parasitophorous vacuole membrane and diffuse within the erythrocyte cytoplasm before taking up residence at the cell periphery.

Plasmodium falciparum causes one of the most life-threatening infectious diseases of humans. Malaria is estimated to be responsible for up to 2 million deaths per year (34). The pathogenesis of the disease is associated with the intraerythrocytic cycle of the parasite, involving repeated rounds of invasion, growth, and schizogony. The erythrocyte provides a ready source of protein building blocks, but this quiescent cell provides little in the way of cellular architecture, as it possesses no internal organelles and no protein synthesis or trafficking machinery. As the parasite develops, it effectively remodels its adopted home by generating membranous structures outside its own cell and by implementing a complex and unusual system for transporting proteins across the host cell compartment and to its surface. This has led to particular interest in the membrane-bound compartments that appear in the red blood cell (RBC) cytoplasm as the parasite matures.

Once the parasite has invaded a new host cell, it resides within a parasitophorous vacuole (PV). In the ring stage of intraerythrocytic growth, electron microscopy studies have revealed finger-like extensions of the PV membrane (5, 11, 43). These extensions are thought to remain connected to the PV and to develop to form a tubulovesicular network (TVN). As the parasite matures, disk-like structures appear at the RBC periphery, characterized by a translucent lumen and an electron-dense coat of variable thickness (4, 11, 22). These structures are referred to as Maurer's clefts, which is something of a misnomer, as they do not appear to be formed by invagination of the RBC membrane (4, 11, 22), though they often appear to be tethered to the RBC membrane by fibrous connections with the erythrocyte cytoskeleton (7, 22). The origin of the Maurer's clefts is not known, and there is currently some debate as to whether the peripheral Maurer's clefts are independent structures or subdomains of the TVN (24, 30). Recent studies used fluorescence microscopy of cells labeled with lipid probes and electron microscopy of serial sections to examine the structures in the *P. falciparum*-infected RBC cytoplasm (43, 45). These authors postulated that Maurer's clefts and the TVN form part of a continuous meshwork. However, other reports using green fluorescent protein (GFP) chimeras of Maurer's cleft-associated cargo (21, 46) suggest that Maurer's clefts are distinct, independent entities.

An important virulence molecule that is exported to the RBC membrane, via the Maurer's clefts, is *P. falciparum* erythrocyte membrane protein 1 (PfEMP1) (9, 24). PfEMP1 is a transmembrane protein that is presented at the RBC surface, where it mediates adhesion of parasitized RBCs to endothelial cells in various organs (12, 33). The subsequent accumulation of infected RBCs in the microvasculature is a pivotal event in the pathogenesis of falciparum malaria (23). Given the proposed role of Maurer's clefts in PfEMP1 trafficking, it is of some interest that components of the plasmodial protein trafficking machinery have been reported to be exported to these structures (1, 3, 16, 38, 44). Moreover, some Maurer's cleft-associated proteins, such as the ring exported protein 1 (REX1, (15) and *P. falciparum* erythrocyte membrane protein 3 (PfEMP3) (42), show structural similarity to vesicle-tethering proteins. This suggests that the Maurer's clefts may function as a protein-sorting compartment that is exported into the RBC cytoplasm.

* Corresponding author. Mailing address: Department of Biochemistry, La Trobe University, Melbourne 3086, Australia. Phone: 61-3-94791375. Fax: 61-3-94792467. E-mail: L.Tilley@latrobe.edu.au.

† Supplemental material for this article may be found at http://mcb.asm.org/.

A series of integral membrane proteins have been shown to be resident at the Maurer's clefts (24). These include *P. falciparum* skeleton binding protein 1 (PfSBP1) (7), the Maurer's cleft two-transmembrane domain proteins (Pfmc2-tm) (32), and the subtelomeric variable open reading frame (STEVOR) proteins (18). Several novel proteins identified by proteomics analysis (39) are also thought to be Maurer's cleft associated. We recently characterized a Maurer's cleft resident protein referred to as the membrane-associated histidine-rich protein 1 (MAHRP1) (37). MAHRP1 is a protein with a predicted molecular mass of 28.9 kDa. The C-terminal domain of MAHRP1 in 3D7 has a histidine content of almost 30% and contains six tandem repeats of the amino acid sequence DHGH, with additional preceding DH repeats.

Recent work (17, 26) has identified a pentameric vacuolar transit sequence/protein export element (VTS/PEXEL motif) in the N-terminal region of exported proteins that is required for transport across the PV membrane. The knob-associated histidine-rich protein, KAHRP, and many other exported proteins possess a highly conserved VTS/PEXEL motif, while a related translocation motif appears to be important for trafficking of PfEMP1 across the PV membrane. MAHRP1 does not contain a sequence that conforms to the criteria used to define the VTS/PEXEL motif, indicating that this resident protein may be trafficked to the RBC cytoplasm via a different route.

Despite the importance of the Maurer's clefts as an intermediate compartment in the delivery of PfEMP1, little is known about the molecular processes that generate these structures and the signals that direct resident proteins to this compartment. In this study, we have generated *P. falciparum* transfectants expressing GFP chimeras of MAHRP1 to dissect the domains needed for correct trafficking. The data suggest that MAHRP1 is trafficked through the parasite ER to the PV membrane. MAHRP1 is then incorporated into small foci (presumably nascent Maurer's clefts) that extend from the PV/TVN prior to transfer to the cell periphery.

MATERIALS AND METHODS

Materials. Rabbit antiserum recognizing GFP and REX1 was kindly donated by Mike Ryan, La Trobe University, Australia, and Paula Hawthorne, Queensland Institute of Medical Research, Australia. Preparation of an antiserum recognizing the PfEMP1 cytoplasmic domain will be described elsewhere (13). Mouse anti-MAHRP1 serum was generated as described previously (37). Mouse antibodies recognizing GFP were obtained from Roche. BODIPY-TR-ceramide was obtained from Molecular Probes Pty Ltd. The pARL1a vector was generated as described previously (10).

Plasmid constructs and transfection of *P. falciparum*. *MAHRP1*$_{1\text{-}249}$, *MAHRP1*$_{1\text{-}105}$, *MAHRP1*$_{106\text{-}124}$, *MAHRP1*$_{125\text{-}249}$, and *MAHRP1*$_{106\text{-}249}$ were cloned into vector pHH2 (31) and then subcloned into pARL1a (10), which had been modified to contain the *GFP* coding region and additional cloning sites (pARL1mGFPmT; kindly generated by A. Adisa, La Trobe University). Briefly, constructs were PCR amplified using primers (see Table I at http://www.latrobe.edu.au/biochemistry/labs/tilley/SuppS1T1T2.html) incorporating ApaI and AflII sites and cloned into the vector pARL1mGFPmT. *P. falciparum*-infected RBCs (ring stage, 3D7 strain) were transfected with 100 μg plasmid DNA and cultured in the presence of 10 nM WR99210, a plasmodial dihydrofolate reductase inhibitor (31). Parasites expressing the GFP chimeric proteins were obtained 20 to 35 days after transfection and thereafter remained close to 100% positive for GFP expression when maintained in the presence of 10 nM WR99210.

Western blot analysis of transfectants. Asynchronous *P. falciparum*-infected RBCs were purified by magnetic sorting (Miltenyi Biotec). Protein samples were subjected to sodium dodecyl sulfate-polyacrylamide gel electrophoresis (12.5% acrylamide), transferred to a nitrocellulose membrane (Hybond-C extra; Amersham Biosciences) for 1.5 h using a Trans-Blot semidry electroblotter (Bio-Rad), and probed with antiserum followed by alkaline phosphatase-conjugated secondary antibodies (Sigma). The membrane was developed in 20 ml of Tris buffer containing 200 μl of 5-bromo-4-chloro-3-indolyl phosphate (15 mg/ml) and 200 μl of nitroblue tetrazolium (30 mg/ml in 70% dimethylformamide). Antibodies for immunoblot analyses were used at the following dilutions: mouse anti-MAHRP1, 1:500; mouse anti-GFP, 1:2,000; goat anti-mouse immunoglobulin G (IgG), 1:20,000.

Fluorescence microscopy and localization studies using indirect immunofluorescence. Fluorescence microscopy was performed using either an Olympus BX50 epifluorescence microscope with 4′,6′-diamidino-2-phenylindole, fluorescein, and rhodamine filter cubes or an inverted Leica TCS-SP2 confocal microscope using ×100 oil immersion objectives (1.4 numerical aperture). In the latter case, argon ion (488 nm) and helium-neon (543 nm) laser lines were employed with the appropriate dichroic filters, and emission wavelengths were selected as previously described (2). Parasitized RBCs expressing MAHRP1-GFP were mounted wet on a glass slide, covered by a glass coverslip, sealed, and imaged within 20 min at ambient temperature (maintained at 20°C).

BODIPY-ceramide was used to label parasitized RBCs as described previously (2). Briefly, parasitized RBCs were resuspended in complete medium (5% parasitemia, 10% hematocrit) and incubated in the presence of 1 μM BODIPY-TR-ceramide at 37°C for 60 min, and then they were washed three times in complete medium and examined by fluorescence microscopy. Serial optical sections (~0.1 to 0.2 μm per section) of GFP- and/or BODIPY-labeled cells were used to generate average maximum-projection three-dimensional (3-D) reconstructions using either the Leica SP2 imaging software or NIH ImageJ (http://rsb.info.nih.gov/ij).

For indirect immunofluorescence microscopy, infected RBCs were smeared onto glass slides and fixed in ice-cold acetone:methanol (1:1, vol/vol) for 10 min. Slides were probed with one of the following primary and secondary antibodies: mouse anti-MAHRP-1c (1:100), rabbit anti-PfEMP1 (1:200), rabbit anti-REX1 (1:1,000), rabbit anti-GFP (1:100), fluorescein isothiocyanate-conjugated anti-rabbit immunoglobin G (IgG; 1:50), and Alexa 568-conjugated anti-mouse IgG (1:200). The slides were mounted in 90% glycerol containing 0.05% *N*-propyl gallate (Sigma) to reduce bleaching.

Electron microscopy. Isolated A4 strain-parasitized RBCs were permeabilized with saponin (36) and incubated with rotation at 37°C with a 1:100 dilution of anti-MAHRP1 serum in RPMI medium with protease inhibitors, followed by 5 nm gold-labeled goat anti-mouse IgG (BioCell). Samples were postfixed with 4% glutaraldehyde in 0.1 M sodium phosphate buffer, pH 7.2, treated with osmium tetroxide, dehydrated, and embedded in epoxy resin. Thin sections were stained with uranyl acetate and lead citrate before examination in a Joel 1200EX transmission electron microscope.

Fluorescence recovery after photobleaching. The general theory and practice of photobleaching measurements has been described elsewhere (19). RBC suspensions (~30% hematocrit) were placed under number 1.5 coverslips, sealed with petroleum jelly, and viewed on an inverted Leica TCS SP2 confocal microscope with a 100× oil immersion objective (1.4 numerical aperture). Images (8 or 12 bit, typically 256 by 256 pixels) were obtained using the 488-nm line of an argon ion laser, and the fluorescence collected through a long-pass 495-nm filter before wavelengths of 500 to 560 nm was selected using the instrument's software. To minimize photobleaching during image acquisition and to maximize the fluorescence signal, the confocal pinhole was opened (3.3 Airy units), the photomultiplier gain was set to high levels, and the laser intensity was minimized to achieve less than 2% bleaching per image. A typical photobleaching measurement comprised two prebleach images to assess the degree of bleaching during image acquisition, a 100- to 1,000-ms spot irradiation of a defined point with the unattenuated laser, and a series of postbleach images. The first postbleach image was obtained immediately after the bleach pulse and is defined as postbleach time zero. Image processing, including background correction, smoothing, and image analysis were performed as described previously (2).

RESULTS

Full-length MAHRP1-GFP is expressed in transfected *P. falciparum*. The MAHRP1 protein sequence (3D7 strain) is shown in Fig. 1a. Exon 1 of the *MAHRP1* gene encodes the first 130 amino acids of the protein, including the 19-amino-acid transmembrane domain and the beginning of the carboxy-terminal domain. Residues 125 to 249 comprise the histidine-rich C-terminal domain. We have generated a chimera comprising

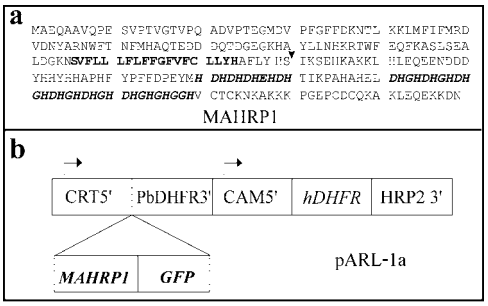

FIG. 1. Organization of the MAHRP1 sequence and transfection construct. (a) *P. falciparum* 3D7 MAHRP1 amino acid sequence (accession no. AAQ63567; MAL 13P1.413). The transmembrane domain and C-terminal histidine-rich repeats are highlighted in boldface and boldface italics, respectively. The exon boundary site is shown with an arrowhead. (b) Schematic diagram of the pARL1a vector showing insertion of the *MAHRP1* sequence upstream of the *GFP* coding region. The plasmid contains a human dihydrofolate reductase (hDHFR) selection cassette. CRT, chloroquine resistance transporter; CAM, calmodulin; HRP2, histidine-rich protein 2.

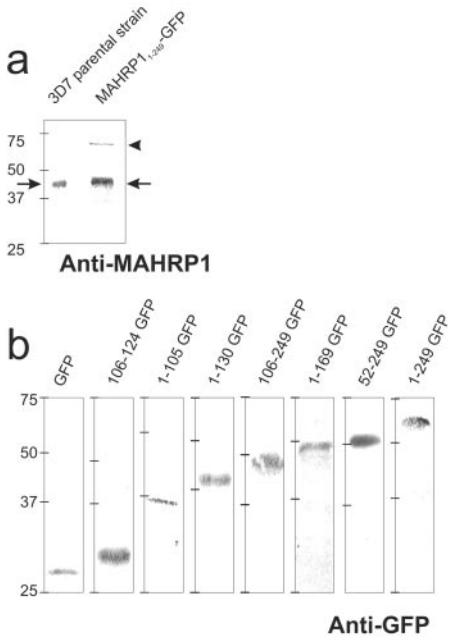

FIG. 2. Western blot analysis of parasite proteins showing expression of MAHRP1-GFP chimeras. (a) *P. falciparum* parental 3D7-infected RBCs ($\sim 5 \times 10^7$ parasites) and $MAHRP1_{1\text{-}249}$-GFP transfectants ($\sim 10^8$ parasites) were subjected to Western blot analysis and probed with anti-MAHRP1 mouse serum. Endogenous MAHRP1 is indicated with an arrow. $MAHRP1_{1\text{-}249}$-GFP is indicated with an arrowhead. (b) Total protein extracts from the different transfectants were subjected to Western blot analysis and probed with anti-GFP antibodies. The predicted sizes of the fusion proteins are given in Table II at http://www.latrobe.edu.au/biochemistry/labs/tilley/SuppS1T1T2.html.

the sequence coding for full-length MAHRP1 linked to the 5′ end of sequence encoding GFP. The full-length *MAHRP1*$_{1\text{-}249}$*-GFP* chimera was inserted into the transfection vector pARL1a (10) under the control of the *PfCRT 5′* region (Fig. 1b). *PfCRT 5′* is a moderate promoter that drives maximal expression in the late ring stages (8), which is similar to the expression profile for MAHRP1 (35).

Asynchronous parasite cultures of parent and transfected lines were subjected to Western blotting and probed with a mouse anti-MAHRP1 antiserum (37) and a rabbit antiserum against GFP. Anti-MAHRP1 recognized a band of approximately 40 kDa (Fig. 2a) in lysates of parental 3D7-infected erythrocytes, as reported previously (37), and an additional band of approximately 70 kDa in the $MAHRP1_{1\text{-}249}$-GFP transfectant (Fig. 2a, arrowhead). The relative intensity of the upper band indicates that MAHRP1-GFP is expressed at lower levels than endogenous MAHRP1. When the blotted lysates were probed with antibodies recognizing GFP, no reactivity was observed in uninfected RBCs or in the 3D7 parent parasites (data not shown), while an approximately 70-kDa protein was observed in $MAHRP1_{1\text{-}249}$-GFP transfectants (Fig. 2b, right lane). Both endogenous MAHRP1 and MAHRP1-GFP migrate with slightly higher apparent molecular masses than predicted (28.9 kDa and 55.9 kDa, respectively). The higher apparent molecular mass is probably due to charged residues in the repeat region of the protein which can cause anomalous migration. There is no evidence for proteolytic processing of either endogenous MAHRP1 or the $MAHRP1_{1\text{-}249}$-GFP chimera.

The $MAHRP1_{1\text{-}249}$-GFP chimera is trafficked to Maurer's clefts via subdomains of the PV membrane. Fluorescence microscopy of live cells has been used to examine the location of $MAHRP1_{1\text{-}249}$-GFP at different stages of growth (Fig. 3). In early-ring-stage parasites (Fig. 3a and b), the MAHRP1-GFP chimera is already present in structures in the host cell cytoplasm that appear to be Maurer's clefts (white arrows). In late ring and early trophozoite stages, some cells showed an accumulation of GFP fluorescence in what appear to be subcompartments associated with the PV or PV membrane (Fig. 3b to d, yellow arrows). In schizont-stage parasites, the structures in the host cell cytoplasm containing MAHRP1-GFP appear to be pushed against the host cell membrane (Fig. 3e), and upon lysis of the host cell membrane (visualized by loss of edge effects in the differential interference contrast [DIC] image) during schizont rupture they remain associated with the lysed RBC membrane (Fig. 3f).

To obtain additional information regarding the organization of the GFP chimera, we generated a 3-D reconstruction from a series of confocal optical slices of the transfectants (see Fig. S2 in the supplemental material for a rotatable image). Distinct compartments containing the GFP chimera are observed close to the periphery of the infected RBC and may be physically tethered to the RBC cytoskeleton (7). In addition, we observed GFP-containing structures located near the surface of the parasite that are visualized as bright puncta and more extended worm-like structures (see Fig. S2 in the supplemental material). We suggest that these may be protein sorting sites or subdomains of the PV, or they may represent nascent Maurer's clefts forming at the PV membrane.

The relationship between the PV-associated (presumably nascent) Maurer's clefts and various membranous structures in the host cell cytoplasm was examined by colabeling the $MAHRP1_{1\text{-}249}$-GFP transfectants with BODIPY-ceramide. This lipid label has previously been used to examine the organization of the PV membrane and TVN (2, 14). Single optical slices through two dual-labeled trophozoite-stage-infected

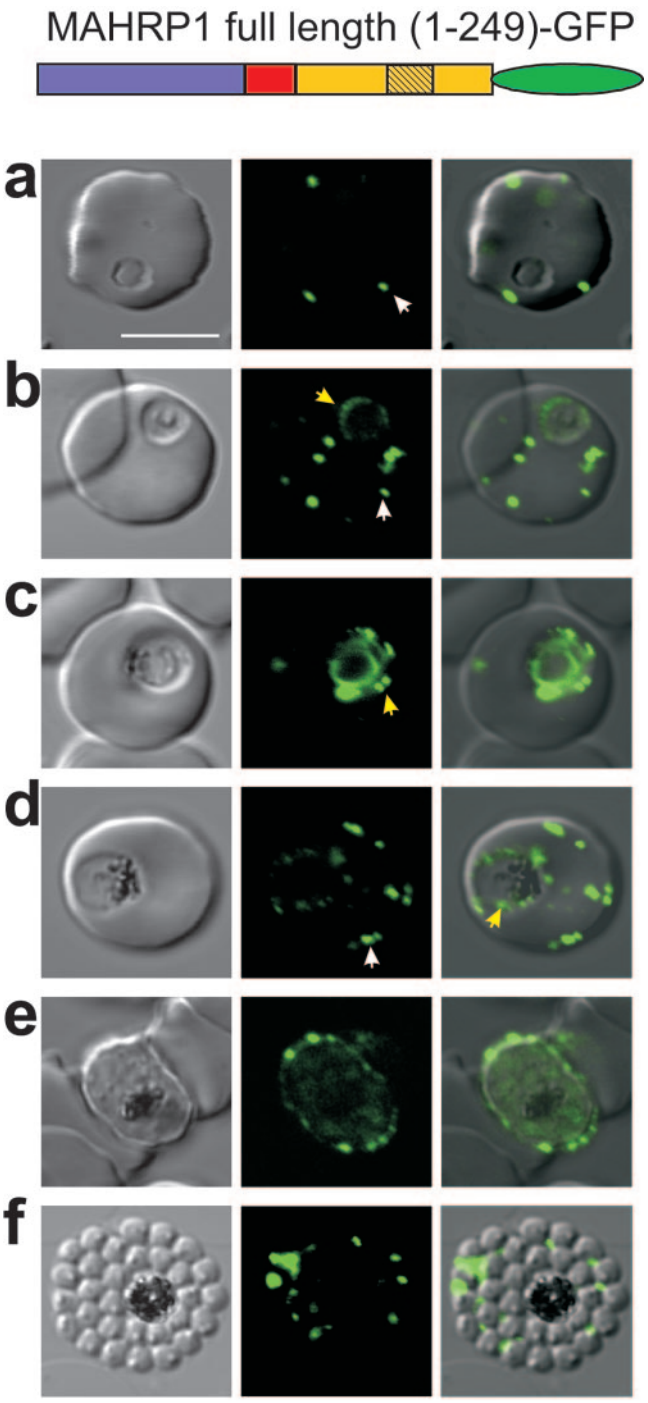

FIG. 3. Expression of MAHRP1$_{1-249}$-GFP at different stages of the intraerythrocytic cycle of *P. falciparum*. The images represent a DIC image, the GFP fluorescence signal, and an overlay of these images. Ring and trophozoite stage parasites (a to d) show puncta of fluorescence in the RBC cytoplasm which appear to represent peripheral Maurer's clefts (white arrows). Some cells (see, e.g., panel c) show a ring of "beads" of fluorescence around the PV. These foci may represent nascent Maurer's clefts (yellow arrows). Mature schizont-stage parasites (e) show flattening of the peripheral Maurer's clefts against the RBC membrane. In a burst schizont (f), the remnant Maurer's clefts remain associated with the lysed host cell membrane. Bar, 5 μm. The intensities of the images were adjusted to optimize the fluorescence signal at each parasite stage.

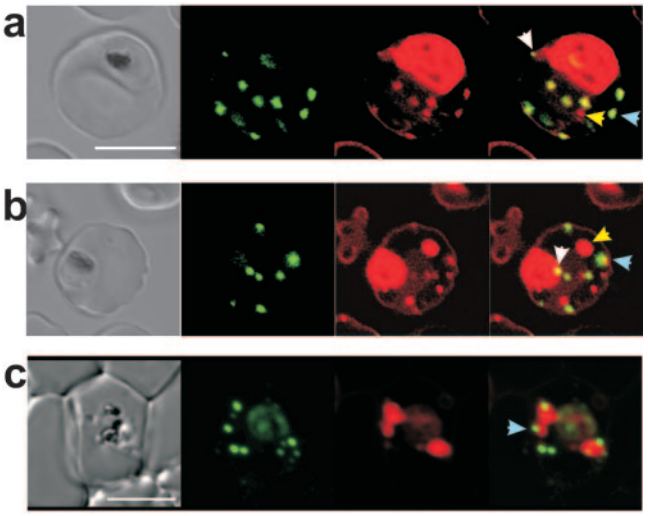

FIG. 4. Dual labeling of MAHRP1$_{1-249}$-GFP transfectants with BODIPY-ceramide. (a to c) The images represent (from left to right) a DIC image, GFP fluorescence, BODIPY-ceramide fluorescence, and an overlay of the GFP (green) and BODIPY-ceramide (red) images. The parasite membranes are intensely labeled with the lipid probe. Some extensions of the PV membrane are dotted with foci of MAHRP1-GFP (white arrows). Some of the BODIPY-labeled structures (probably TVN extensions and buds) are not labeled with GFP (yellow arrows), while others (presumably Maurer's clefts) are labeled with GFP (blue arrows). The fluorescence images in panel c correspond to an average projection generated from a series of optical slices. See Fig. S3 in the supplemental material for a video showing a 3-D rotation. Bar, 5 μm.

RBCs are shown in Fig. 4a and b. BODIPY-ceramide labels the membrane-rich parasite cytoplasm very heavily as well as punctate structures in the RBC cytoplasm. Most of these structures are labeled with both BODIPY-ceramide and GFP (Fig. 4a and b, white and blue arrows) and presumably represent nascent and mature Maurer's clefts. The labeling with BODIPY-ceramide is fairly weak, which may indicate a relatively low lipid content. Some BODIPY-ceramide-labeled structures do not contain MAHRP1$_{1-249}$-GFP (Fig. 4a and b, yellow arrows). These appear to represent a second population of TVN buds and extensions that are distinct from the Maurer's clefts. We have previously reported the budding of regions of the TVN (2). Figure 4c shows an average projection of a cell generated from a series of optical slices. A video showing rotatable images can be found in Fig. S3 in the supplemental material. Rotation of this image reveals what appear to be nascent Maurer's clefts associated with extensions of the PV membrane or TVN (Fig. 4c, blue arrow). Again, the data suggest that MAHRP1$_{1-249}$-GFP collects into subdomains on the PV membrane or TVN.

Immunofluorescence analysis confirms the Maurer's cleft location of MAHRP1-GFP. We have used indirect immunofluorescence microscopy to confirm the subcellular location of MAHRP1$_{1-249}$-GFP in the transfectants. In cells fixed with acetone:methanol (which destroys the endogenous GFP fluorescence), antibodies against GFP gave a pattern of distribution similar to that observed in live cells. The chimera was present in punctate structures in the host cell cytoplasm (Fig. 5a). Dual labeling with an antiserum recognizing endogenous

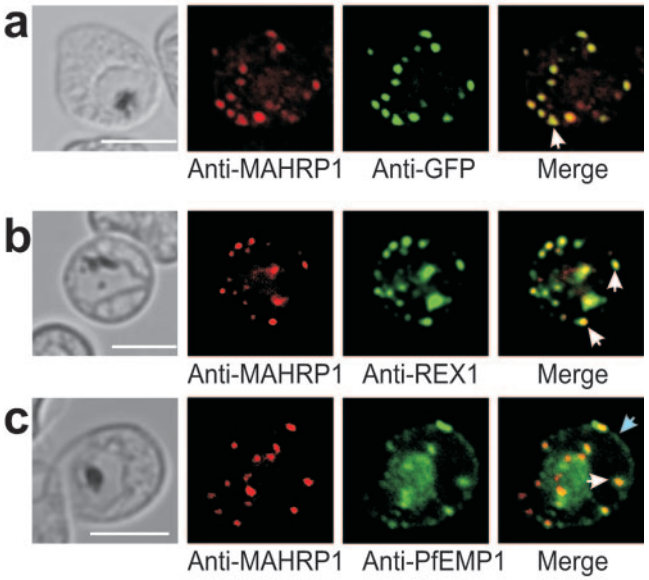

FIG. 5. Immunofluorescence microscopy of MAHRP1$_{1-249}$-GFP. (a) Trophozoite-stage-infected RBC labeled with mouse anti-MAHRP1 antiserum (red) and rabbit anti-GFP antiserum (green). A dual-labeled Maurer's cleft (white arrow) is indicated. (b) Trophozoite stage infected RBC labeled with mouse anti-MAHRP1 (red) and rabbit anti-REX1 (green) antisera. (c) Trophozoite stage infected RBCs labeled with mouse anti-MAHRP1 (red) and rabbit anti-PfEMP1 (green). Overlap of these signals confirms the Maurer's clefts location (white arrow). PfEMP1 is also partly located at the RBC membrane (blue arrow). The bars represent 5 μm.

MAHRP1 showed a very similar pattern, with almost complete overlap of GFP and MAHRP1 in the punctate structures in the RBC cytoplasm (Fig. 5a, white arrow).

To confirm the identity of the punctate compartments in the host cell cytoplasm, we undertook dual labeling with a known Maurer's cleft marker, the ring-stage-exported protein REX1 (Fig. 5b). The complete overlap of these signals (Fig. 5b, white arrows) provides further evidence that these structures are Maurer's clefts. We also examined the profiles of cells labeled with an antiserum against the cytoadherence antigen, PfEMP1. This protein is exported to peripheral Maurer's clefts (Fig. 5c) prior to redistribution to the RBC membrane (Fig. 5c, blue arrow). MAHRP1 is colocalized with PfEMP1 when it is associated with the Maurer's clefts (Fig. 5c, white arrow) and may play an important role in transit of this protein through the Maurer's cleft compartment.

Ultrastructural analysis reveals MAHRP1 organization and orientation at the Maurer's clefts. To examine the exact location of endogenous MAHRP1, we have introduced antibodies against the C-terminal domain of MAHRP1 into saponin-permeabilized infected RBCs using methods developed previously (36). The permeabilized cells were incubated with 5 nm gold-labeled anti-mouse IgG prior to processing for transmission electron microscopy. This allowed us to probe the population of endogenous MAHRP1 in the RBC cytoplasm compartment. Maurer's clefts with electron-dense coats were frequently observed in sections of early trophozoite-stage parasitized RBCs (Fig. 6). The Maurer's clefts were decorated with gold particles that appeared to be concentrated in the central region of the organelle. The fact that the MAHRP1 antibody (which is raised against the C-terminal domain) is able to access its binding epitope in these permeabilized cells and the observation that the particles are largely arrayed at the cytoplasmic surface of the Maurer's clefts indicates that the C terminus (His-rich region) of MAHRP1 is facing the RBC cytoplasm. In a few (<10%) of the labeled cells, it was possible to observe gold particles associated with areas of the PV membrane (Fig. 6b and c, arrowheads). These may represent areas of the PV membrane where MAHRP1 has accumulated prior to the formation of Maurer's clefts.

Part of the N-terminal domain and the transmembrane domain of MAHRP1 are needed for correct trafficking to the Maurer's clefts. MAHRP1 does not contain a sequence that conforms to the criteria used to define the VTS/PEXEL motifs (17, 26), indicating that this resident protein may be trafficked to the Maurer's clefts via a different route to other exported proteins. Alternatively, MAHRP1 may contain an unusual VTS/PEXEL motif or a different export signal. In an effort to determine the regions of the MAHRP1 sequence that are needed for correct trafficking, we have generated transfectants expressing a range of fragments of MAHRP1 appended to GFP and examined their intracellular locations.

When GFP alone is expressed in transfected *P. falciparum*, it is present in the parasite cytoplasm (Fig. 7a; see Fig. S1a at http://www.latrobe.edu.au/biochemistry/labs/tilley/SuppS1T1T2.html). When the N-terminal domain of MAHRP1 was fused to GFP, the chimeric protein appears to remain in the parasite cytoplasm (Fig. 7b; see Fig. S1b at the website listed earlier in this paragraph). By contrast, a GFP fusion protein containing the transmembrane domain of MAHRP1 appeared to enter the endoplasmic reticulum (ER) and to remain in this compartment (Fig. 7c; see Fig. S1c at the website listed earlier in this paragraph). The ER location is indicated by the fact that the protein is located in a compartment that surrounds the nucleus (see Fig. S1c at the website listed earlier in this paragraph). A construct comprising the transmembrane and C-terminal domains also appears to remain trapped in the ER (Fig. 7d; see Fig. S1d at the website listed earlier in this paragraph).

Thus, it appears that the transmembrane domain is needed for the chimera to enter the ER, the first step of the export pathway, but that additional sequence is needed for subsequent steps. Therefore, we generated a chimera with the first 169 amino acids of MAHRP1 (comprising the N-terminal and transmembrane domains and the first 45 amino acids of the C-terminal region) fused to GFP. The fusion protein was successfully exported to the RBC cytoplasm (Fig. 7f) and became associated with the Maurer's clefts. This indicates that the first 169 amino acids are sufficient for correct trafficking and that the His-rich repeats (amino acids 170 to 214) are not needed. A further construct was generated comprising the first 130 amino acids fused to GFP; this is equivalent to the sequence encoded by exon 1 (i.e., up to the sixth amino acid of the C-terminal domain). This fusion protein was partly exported to the RBC cytoplasm and became associated with the Maurer's clefts (Fig. 7e, second row); however, the export process appeared to be less efficient. In this transfectant, a build-up of the fluorescent chimera in what appears to be the ER and structures associated with the PV membrane was frequently ob-

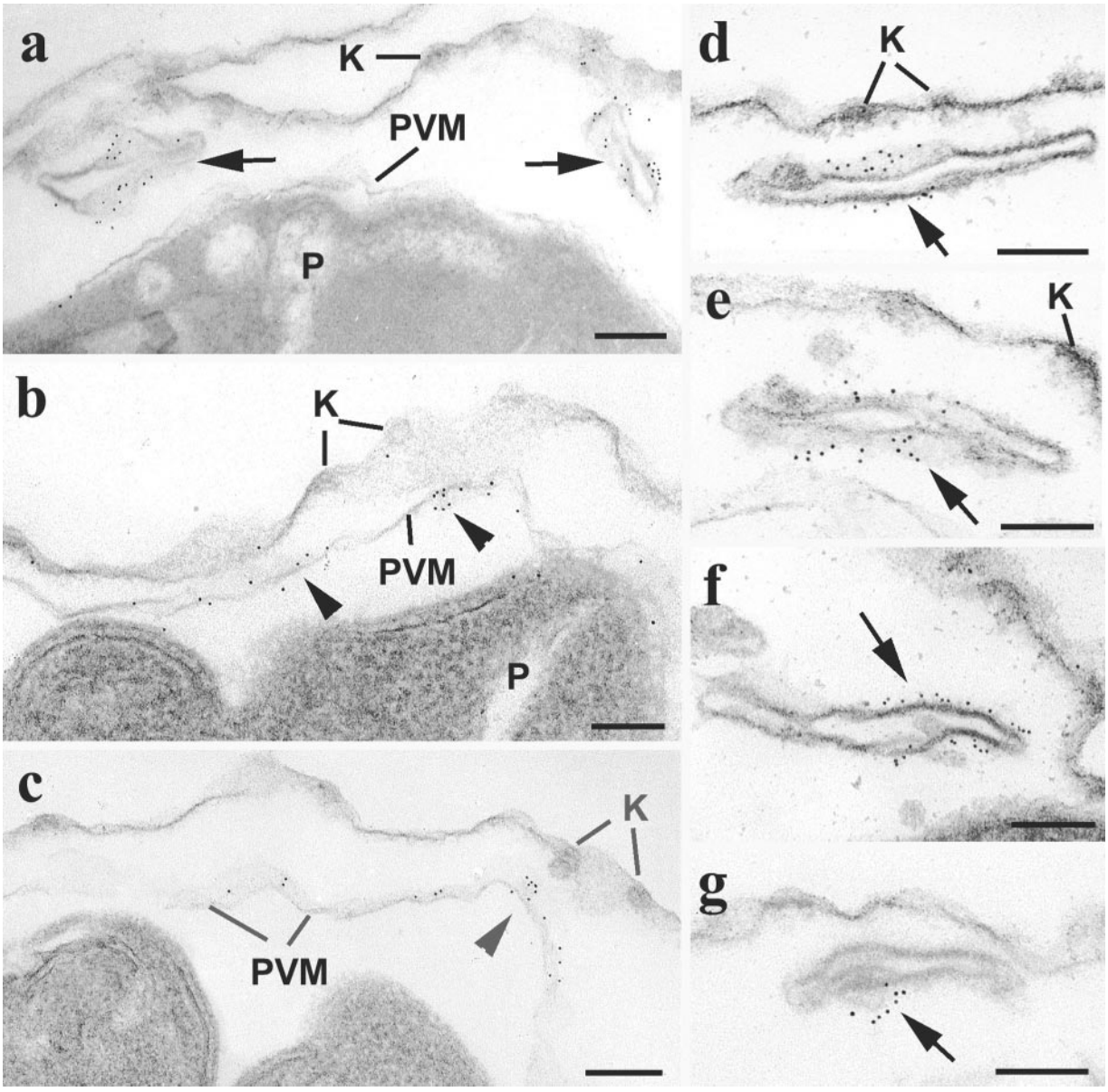

FIG. 6. Transmission electron microscopy of immunogold labeling of MAHRP1 in saponin-permeabilized parasitized RBCs. (a to c) Sections through the periphery of infected RBCs showing labeling of the Maurer's clefts (arrows) with variable labeling of the PV membrane (PVM; arrowheads). In most sections (a), the PVM is unlabeled; however, in a few sections (b and c), there is focal labeling. (d to g) Details of Maurer's clefts showing that the gold particles are mainly located in the central region (arrows). K, knobs; P, parasite. Bars, 100 nm.

served (Fig. 7e, first row). This indicates that information in the first half of the C-terminal domain (amino acids 131 to 169), while not necessary for export, may facilitate delivery to the Maurer's clefts. To assess whether an export signal is present within the sequence close to the N terminus, we generated a further chimera with a truncation of the first 51 amino acids. As shown in Fig. 7g, this chimera is successfully exported to the Maurer's clefts with efficiency similar to that of full-length MAHRP1-GFP (Fig. 7h). This indicates that the second half of the N-terminal domain contains the signal for transfer from the parasite's endomembrane system to the Maurer's clefts. It is important to note that endogenous MAHRP1 was expressed and correctly trafficked to peripheral Maurer's clefts in all transfectants (data not shown).

In some (5 to 10% of cells) of the young trophozoite-stage transfectants expressing the $MAHRP_{1\text{-}130}$-GFP and $MAHRP1_{52\text{-}249}$-GFP constructs, structures were observed that appeared to be Maurer's cleft compartments that had budded from the PV membrane but had not yet become attached to the RBC membrane. Stills of one of these cells taken at different time points are presented in Fig. 8a. Movies showing the movement of untethered clefts in this cell and in some other examples can be found in Fig. S4 of the supplemental material. The occasional observation of these mobile clefts supports the

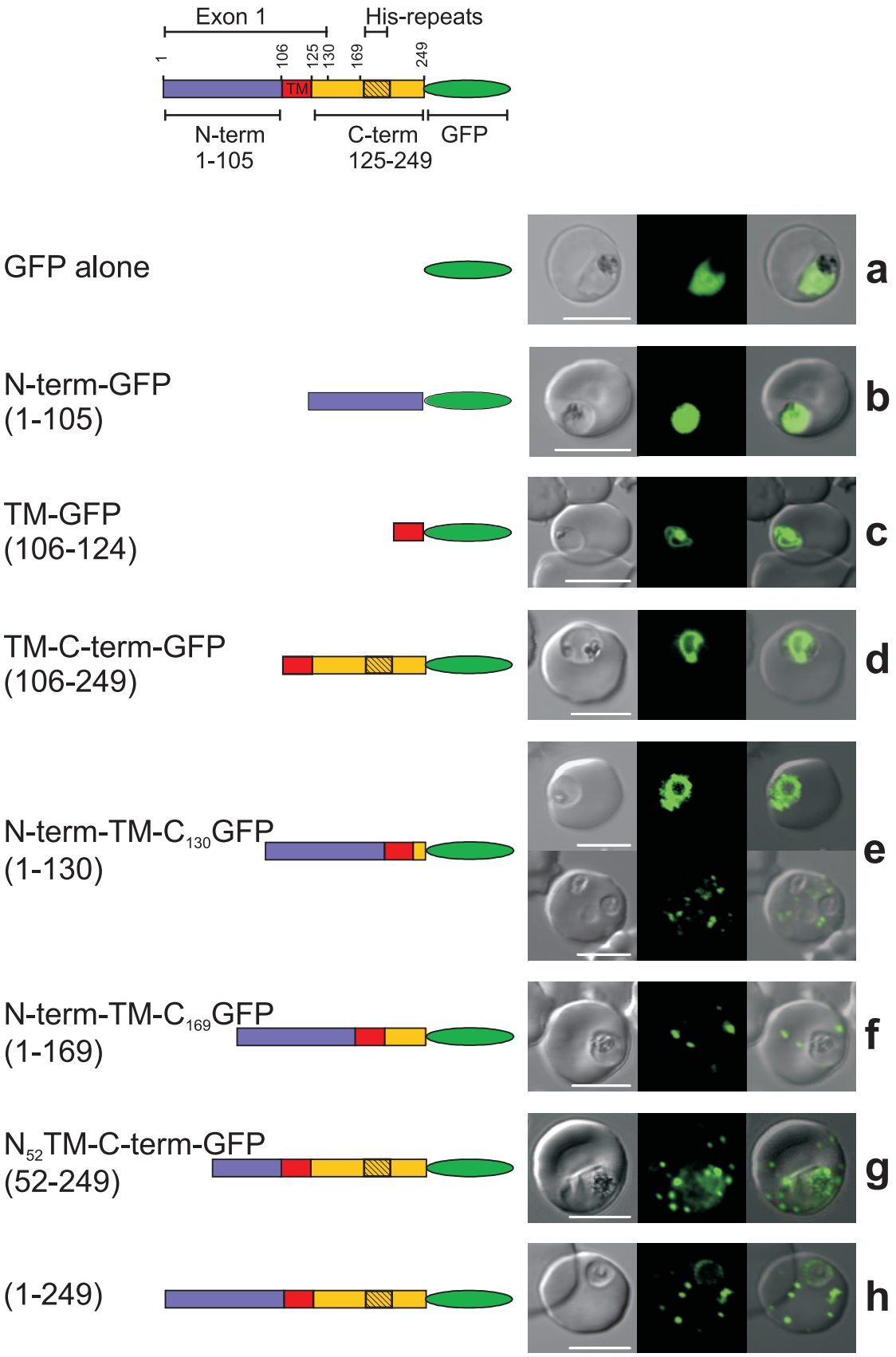

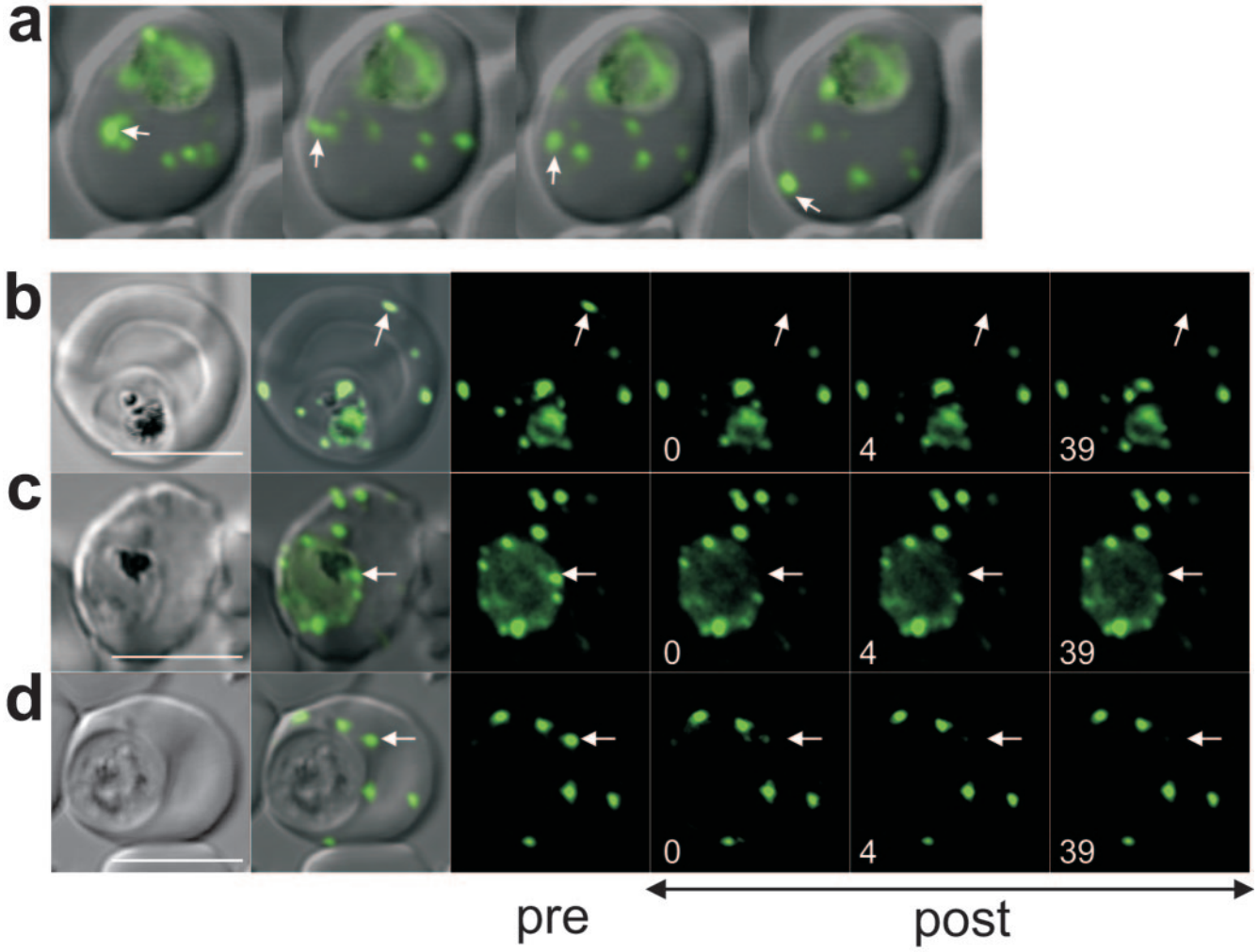

FIG. 8. Molecular organization of GFP chimeras in different compartments. (a) Overlay images of a MAHRP1$_{1\text{-}130}$-GFP transfectant displaying mobile Maurer's clefts taken at consecutive time points. One moving cleft observed over time is indicated with white arrows. A movie of this cell and other examples can be viewed in Fig. S4. The bar represents 5 μm. (b to d) Photobleach analysis. The panels show the DIC images and the prebleach (pre) and postbleach (post) fluorescence images at the times (in seconds) indicated. The position of the bleach pulse is indicated by white arrows. (b) Bleaching of MAHRP1$_{52\text{-}249}$-GFP in a tethered peripheral Maurer's cleft with a 300-ms bleach pulse. There is no recovery of the signal after photobleaching, indicating a physically separate structure. Bleaching of a PV membrane-associated MAHRP1$_{52\text{-}249}$-GFP focal region with 300-ms bleach pulses (c) and a structure in close proximity to the PV membrane with a 200-ms bleach pulse (d). There is no recovery of fluorescence into the bleached areas. Scale bars, 5 μm.

suggestion that Maurer's clefts bud from the PV membrane as preformed structures and then take up residence at the cell periphery.

To determine whether the correct GFP-MAHRP1 fragment chimeras were expressed, we performed Western blot analyses of each of the different transfectants. Total parasite extracts were blotted and probed with anti-GFP (Fig. 2b). The immunoreactive bands have molecular weights that are close to or (for parasite lines expressing products incorporating the C-terminal repeats) slightly higher than the predicted molecular

FIG. 7. Dissecting the domains required for correct trafficking of MAHRP1 to the Maurer's clefts. At the top is a schematic representation of the MAHRP1 full-length protein with its three domains (N terminal [N-term], transmembrane [TM], and C terminal [C-term]), with numbering of key amino acids and the GFP. Transfected *P. falciparum*-expressing GFP linked to different domains of MAHRP1 were examined by confocal fluorescence microscopy. (a) GFP alone is evenly distributed throughout the parasite cytoplasm. A chimera of the N-terminal region (amino acids 1 to 105) (b) also appears to be restricted to the parasite cytoplasm. Chimeras of the transmembrane domain of MAHRP1 (106 to 124) (c) and of the transmembrane domain and C-terminal region of MAHRP1 (amino acids 106 to 249) (d) appear to be located in the parasite's endomembrane system. A chimera of the N-terminal region and transmembrane domain of MAHRP1 (amino acids 1 to 130) (e) is partly exported to the RBC cytoplasm but in some cells accumulates within the parasite. A chimera containing amino acids 1 to 169 (f), a deletion of the first 51 amino acids (g), and full-length MAHRP1-GFP (h) are efficiently exported to the RBC cytoplasm. Bars, 5 μm.

weights. Predictions of the expected sizes for each of the fusion proteins are given in Table II at http://www.latrobe.edu.au/biochemistry/labs/tilley/SuppS1T1T2.html. In each case a single band was observed, indicating that there is no proteolytic processing of the chimeras.

Exported MAHRP1-GFP becomes tightly associated with the Maurer's clefts. We performed photobleaching studies (19) of Maurer's cleft-associated full-length MAHRP1-GFP ($MAHRP1_{1-249}$-GFP) and of the chimera with the first 51 amino acids deleted ($MAHRP1_{52-249}$-GFP) to examine the physical organization of the fusion proteins and the connectivities of the compartments in which they are located. We first examined whether the population of the fusion proteins associated with the Maurer's cleft is tightly associated with these structures or rapidly exchanging with a cytoplasmic pool which, although not readily visible, may be present. Selective bleaching of $MAHRP1_{52-249}$-GFP associated with a tethered cleft at the periphery of the RBC was achieved with a 0.3-s exposure to a laser pulse (Fig. 8b, white arrow). There was no recovery of fluorescence onto the Maurer's clefts within the time scale examined. The same result was obtained for full-length $MAHRP_{1-249}$-GFP (data not shown). This indicates that the MAHRP1-GFP fusion proteins are tightly bound at the Maurer's clefts and that there is no connectivity between different Maurer's clefts, or at least no exchange of the chimeras. The data are consistent with the suggestion that the fusion proteins are embedded in the Maurer's cleft membrane and that the Maurer's clefts lack a direct physical connection to other membrane-bound structures.

We also examined the physical organization of the MAHRP1-GFP fusion proteins within the fluorescent puncta that are associated with the PV membrane. We bleached compartments that were close to the parasite surface (Fig. 8c, arrow) or seemed to be in the process of budding from the PV membrane (Fig. 8d, arrow). In both cases the bleach profile was restricted to the region to which the laser pulse was applied, and there was no fluorescence recovery into the bleached area. This indicates that even at the PV membrane, the MAHRP1-GFP-containing compartments are physically separate structures. The lateral segregation of MAHRP1-GFP molecules into nonexchanging subdomains of the PV membrane is consistent with the suggestion that these domains are sites of formation of Maurer's clefts.

Taken together with the BODIPY-ceramide dual-labeling experiments, the movies of untethered clefts, and the fact that we did not observe any small MAHRP1-containing vesicles in the RBC cytoplasm, the data for bleaching of the proximal (presumably nascent) and peripheral (presumably mature) Maurer's clefts suggest that these compartments are assembled at the PV membrane and trafficked as "ready-made" structures to the periphery of the RBC. However, it remains formally possible that MAHRP1 is packaged into small vesicles (that are transient and difficult to observe) that subsequently fuse with mature clefts.

DISCUSSION

The malaria parasite establishes a novel and unusual secretory pathway in the cytoplasm of its erythrocytic host. Unable to commandeer any trafficking machinery from its host cell, the parasite needs to establish both rolling stock and transport routes for transfer of material across the host cell cytoplasm. A major feature of the infected RBC cytoplasm is the appearance of densely coated, saucer-shaped structures, known as Maurer's clefts, that are proposed to function as a transit station or sorting depot for proteins en route to the RBC membrane (9, 24). Because of their presumed importance in the trafficking of PfEMP1 and other exported proteins, the Maurer's clefts are currently being studied in some detail.

MAHRP1 is a Maurer's cleft resident protein that may be involved in the formation of this important organelle or in the transit of PfEMP1 through this compartment (37). It is a small protein with no significant homology to any known sequence. It has no predicted N-terminal signal sequence but has a 19-amino-acid Phe-rich transmembrane domain. In this work, we have generated transfected parasites expressing fusions of either full-length MAHRP1 or a series of MAHRP1 fragments in an effort to dissect the pathway for trafficking to the Maurer's clefts. Indeed, full-length MAHRP1-GFP is trafficked to the host cell cytoplasm, where it occupies the same compartments as endogenous MAHRP1.

We have used saponin permeabilization of infected RBCs as a means of introducing gold-labeled antibodies that recognize the C-terminal domain of endogenous MAHRP1. Transmission electron micrographs of these labeled cells revealed Maurer's clefts decorated with gold particles on their cytoplasmic surface. This indicates that the C-terminal domain of MAHRP1 is exposed to the RBC cytoplasm. This is in agreement with the prediction of the PSORT algorithm (27), which suggests a type Ib orientation for MAHRP1. Another Maurer's cleft resident, PfSBP1, is also predicted to be a type Ib protein and is known to be oriented with its C-terminal region facing the RBC cytoplasm (7).

MAHRP1 appears to be concentrated in the central region of the Maurer's clefts. Permeabilization of parasitized RBCs has previously been used to introduce antibodies against the cytoplasmic domain of PfEMP1 into the host cell cytoplasm. A similar distribution was observed for PfEMP1, although PfEMP1 was also observed associated with fibrous extensions of the Maurer's clefts (22). It is possible that MAHRP1 plays a role in docking PfEMP1 complexes onto the Maurer's cleft membrane or helping to insert PfEMP1 into a membrane environment. In contrast, electron microscopy analysis of PfSBP1 revealed preferential labeling of the rims of the Maurer's clefts (7). These data suggest that the Maurer's clefts could contain subcompartments that perform different functions.

The availability of transfectants expressing MAHRP1-GFP offers the possibility of following the pathway for trafficking of this protein and potentially for observing the mode of formation of Maurer's clefts. In some transfected cells, we observed an accumulation of MAHRP1-GFP in foci associated with the PV membrane, presumably en route to the host cell cytoplasm. We have used colabeling with BODIPY-ceramide and 3-D image reconstruction to examine the organization of MAHRP1-GFP within the PV membrane. The lipid probe labels the endomembrane system of the parasite as well as the PV membrane/TVN extensions and small discrete structures in the host cell cytoplasm. Some of the membranous structures in the RBC cytoplasm (presumably the Maurer's clefts) are labeled with MAHRP1-GFP, while some are not; these could represent

regions of the TVN that have budded into the RBC cytoplasm but are distinct from Maurer's clefts, as has been reported previously (2).

We were particularly interested in the foci of MAHRP1-GFP that appear to accumulate in regions of the PV membrane and in tubulovesicular extensions. These foci are reminiscent of ER "exit complexes" (28), and we propose that this accumulation event represents the genesis of the Maurer's clefts. The tendency of MAHRP1-GFP to concentrate into particular subdomains of the PV/TVN membranes may be due to self association or to association with other Maurer's cleft resident proteins. In some of the transfectants expressing truncated MAHRP1-GFP, we occasionally observed an accumulation of mobile clefts that appeared to have budded from the PV membrane. These data suggest that clefts that are released from the PV membrane diffuse within the RBC cytoplasm until they become tethered to the RBC membrane.

Florescence recovery after photobleaching can be used to provide information on the organization and dynamics of GFP chimeras in transfected malaria parasites (2, 19, 46). We have used confocal microscope-based photobleaching protocols to probe the physical organization of MAHRP1-GFP en route to the Maurer's clefts. MAHRP1 chimeras that are present in the peripheral Maurer's clefts or in foci at the PV membrane appear to represent distinct nonconnected structures. Bleaching of one focal aggregate did not deplete the fluorescence from other regions, indicating that the proteins are not able to move laterally within the membrane or that the separate foci are not connected by a fluid continuum. We have previously reported that soluble GFP-labeled proteins in the PV lumen can be restricted to subcompartments within the PV, forming a so-called necklace of beads around the parasite surface (2, 46). The integral membrane protein, exported protein-1 (Exp1), and early transcribed membrane protein, ETRAMP, have also been reported to undergo lateral segregation into different regions of the PV membrane (36). Thus, our current findings reinforce the idea that the PV contains separate subcompartments.

A recent study postulated that Maurer's clefts and the TVN form part of a continuous network (45). An earlier immunofluorescence microscopy study employing an antibody against protein Ag45 also led to the conclusion that Maurer's clefts are subcompartments of the TVN (6). Our results indicate that the peripherally located Maurer's clefts are not interconnected, or at least that a physical barrier prevents the diffusion of GFP chimeras between adjacent Maurer's clefts. Similarly, we find no evidence for continuity of the peripheral Maurer's cleft structures with the PV membrane. However, the nascent Maurer's clefts do appear to form subdomains of the PV/TVN membrane, which is consistent with the interconnected structures observed by other workers (6, 43). This work therefore serves to clarify the apparent differences between these different studies.

In an effort to determine the domains that are responsible for correct trafficking of MAHRP1 to the Maurer's clefts, we generated transfectants expressing subdomains of MAHRP1 linked to GFP. When the N-terminal domain was used alone, the chimera remained trapped in the parasite cytoplasm. Constructs containing the transmembrane domain, either alone or combined with the C-terminal domain, entered the ER but were unable to progress beyond this compartment. By contrast, a construct comprising the first 130 amino acids of MAHRP1 (N-terminal and transmembrane domains and the first 6 amino acids of the C-terminal region) was trafficked to the Maurer's clefts, albeit with lower efficiency, while a construct with the first 169 amino acids was trafficked with similar efficiency to the full-length (amino acids 1 to 249) construct. Similarly, a construct comprising the second half of the N-terminal domain plus the transmembrane and C-terminal domains (amino acids 52 to 249) was efficiently trafficked to the Maurer's clefts. Taken together, these data indicate that the information required for directing MAHRP1 to its final destination is contained within the second half of the N-terminal domain and that the transmembrane domain is required for entry into the ER.

The sequence information directing MAHRP1 trafficking appears to be different from that needed for correct export of STEVOR, another Maurer's cleft-associated protein (29). Most exported plasmodial proteins, including the STEVOR family, are encoded by 2-exon genes and possess both a hydrophobic signal sequence, encoded by the first exon, and an RxLxE/Q sequence, close to the start of the second exon (17, 26). PfEMP1 represents a second class of exported proteins. It lacks an N-terminal hydrophobic signal sequence, and its export is thought to be determined by a related sequence, AKHLLDRLG (26) or FFRWFSEWSE (17), in the N-terminal region of the protein. MAHRP1 has a sequence (comprising amino acids 87 to 99) which has a charge distribution similar to that of the PfEMP1 VTS/PEXEL. It is possible that this region represents the signal directing forward transit of this protein.

Charge differences between the N- and C-terminal regions are important in determining the topology of integral membrane proteins (40). It is possible that charge differences contribute to the signal information needed for correct MAHRP1 trafficking. The N-terminal domain of MAHRP1 has a theoretical pI of 4.73, while the C-terminal domain has a pI of 6.19. This charge difference is responsible for the type Ib prediction (C terminus cytoplasmic) using the PSORT algorithm (27). This charge difference is lower in some of the constructs generated in this study, but for each of the exported chimeras it is still sufficient to predict a type Ib orientation. Indeed, a lesser charge difference may explain why $MAHRP1_{1\text{-}130}$-GFP is exported somewhat less efficiently. Interestingly, PfSBP1, another integral membrane protein that is directed to the Maurer's cleft, has a similar charge differential between the N- and C-terminal domains.

PfEMP1 is thought to insert into a membrane environment when it reaches the Maurer's clefts prior to transit to the RBC membrane (21). It is interesting to note that while the cytoplasmic domains of MAHRP1 and PfSBP1 are relatively basic, the cytoplasmic domain of PfEMP1 is highly acidic. KAHRP and PfEMP3 are also transiently associated with the Maurer's clefts before redistribution to the cytoplasmic face of the RBC membrane (42, 46). The regions responsible for Maurer's cleft binding in KAHRP and PfEMP3 have been defined (20, 25, 46). For PfEMP3, residues 120 to 500 are sufficient for tight Maurer's cleft binding (20); this region has a pI of 9.21. KAHRP residues 60 to 120, with a pI of 7.07, are sufficient for weak binding to the Maurer's clefts (25, 46). However, stronger

interaction with the cytoplasmic domain of PfEMP1 requires the 5′ and 3′ repeat regions (41); the pI for this region of the protein is 9.64. Positively charged regions in the cytoplasmic domains of MAHRP1 and PfSBP1 may interact with the highly acidic cytoplasmic domain of PfEMP1 and facilitate the process of insertion of PfEMP1 into the Maurer's cleft membrane. It is possible that subsequent charge interactions with proteins such as KAHRP and PfEMP3 may assist in separating PfEMP1 into a separate compartment within the Maurer's cleft and facilitate forward transit of this protein.

Taken together with data from other studies, our work suggests a possible model for trafficking of proteins to the RBC membrane. Maurer's cleft resident proteins, such as MAHRP1, are expressed in the ring stage and are likely to be needed for the genesis of the parasite's extracellular secretory pathway. Our current data provide evidence that MAHRP1 is directed into the ER and, somehow, transferred from the parasite plasma membrane to the PV/TVN membrane. Here, MAHRP1 appears to coalesce into small foci that may represent nascent Maurer's clefts. The Maurer's clefts appear to bud from the PV/TVN membrane before docking at sites near the RBC periphery, although it remains possible that small vesicle-mediated trafficking is also involved. The insertion of PfEMP1 may take place at either nascent or peripheral Maurer's clefts. Electrostatic interactions may facilitate the docking and sorting functions within this compartment.

In summary, we have provided the first insights into the formation of Maurer's clefts and determined regions of MAHRP that are needed for trafficking to these important subcellular structures. Strategies that inhibit the formation of the Maurer's clefts or the insertion of proteins into this compartment could provide a means of interfering with the display of virulence epitopes at the surface of infected RBCs.

ACKNOWLEDGMENTS

This work was supported by the National Health and Medical Research Council, Australia, and the Swiss National Science Foundation (grant number 3100A0-104043/1). D.J.P.F. is supported by an equipment grant from the Wellcome Trust.

Expert technical assistance was provided by Emma Fox. We thank Selina Bopp and Christian Flück for constructive discussions and Paula Hawthorne, QIMR, and Mike Ryan, La Trobe University, Australia, for providing antibodies.

REFERENCES

1. **Adisa, A., F. R. Albano, J. Reeder, M. Foley, and L. Tilley.** 2001. Evidence for a role for a *Plasmodium falciparum* homologue of Sec31p in the export of proteins to the surface of malaria parasite-infected erythrocytes. J. Cell Sci. **114:**3377–3386.
2. **Adisa, A., M. Rug, N. Klonis, M. Foley, A. F. Cowman, and L. Tilley.** 2003. The signal sequence of exported protein-1 directs the green fluorescent protein to the parasitophorous vacuole of transfected malaria parasites. J. Biol. Chem. **278:**6532–6542.
3. **Albano, F. R., A. Berman, N. La Greca, A. R. Hibbs, M. Wickham, M. Foley, and L. Tilley.** 1999. A homologue of Sar1p localises to a novel trafficking pathway in malaria-infected erythrocytes. Eur. J. Cell Biol. **78:**453–462.
4. **Atkinson, C. T., M. Aikawa, G. Perry, T. Fujino, V. Bennett, E. A. Davidson, and R. J. Howard.** 1988. Ultrastructural localization of erythrocyte cytoskeletal and integral membrane proteins in *Plasmodium falciparum*-infected erythrocytes. Eur. J. Cell Biol. **45:**192–199.
5. **Bannister, L. H., J. M. Hopkins, R. E. Fowler, S. Krishna, and G. H. Mitchell.** 2000. A brief illustrated guide to the ultrastructure of *Plasmodium falciparum* asexual blood stages. Parasitol. Today **16:**427–433.
6. **Behari, R., and K. Haldar.** 1994. *Plasmodium falciparum*: protein localization along a novel, lipid-rich tubovesicular membrane network in infected erythrocytes. Exp. Parasitol. **79:**250–259.
7. **Blisnick, T., M. E. Morales Betoulle, J. Barale, P. Uzureau, L. Berry, S. Desroses, H. Fujioka, D. Mattei, and C. Braun Breton.** 2000. Pfsbp1, a Maurer's cleft *Plasmodium falciparum* protein, is associated with the erythrocyte skeleton. Mol. Biochem. Parasitol. **111:**107–121.
8. **Bozdech, Z., J. Zhu, M. P. Joachimiak, F. E. Cohen, B. Pulliam, and J. L. DeRisi.** 2003. Expression profiling of the schizont and trophozoite stages of *Plasmodium falciparum* with a long-oligonucleotide microarray. Genome Biol. **4:**R9.
9. **Cooke, B. M., K. Lingelbach, L. Bannister, and L. Tilley.** 2004. Protein trafficking in *Plasmodium falciparum*-infected red blood cells. Trends Parasitol. **20:**581–589.
10. **Crabb, B. S., M. Rug, T. W. Gilberger, J. K. Thompson, T. Triglia, A. G. Maier, and A. F. Cowman.** 2004. Transfection of the human malaria parasite *Plasmodium falciparum*. Methods Mol. Biol. **270:**263–276.
11. **Elford, B. C., G. M. Cowan, and D. J. Ferguson.** 1995. Parasite-regulated membrane transport processes and metabolic control in malaria-infected erythrocytes. Biochem. J. **308:**361–374.
12. **Flick, K., and Q. Chen.** 2004. var genes, PfEMP1 and the human host. Mol. Biochem. Parasitol. **134:**3–9.
13. **Frankland, S., A. Adisa, P. Horrocks, T. Taraschi, T. Schneider, S. R. Elliot, S. J. Rogerson, K. E. A. F. Cowman, C. I. Newbold, and L. Tilley.** 2006. Delivery of the malaria virulence protein, PfEMP1, to the erythrocyte surface requires cholesterol-rich domains. Eukaryot. Cell **5:**849–860.
14. **Haldar, K., L. Uyetake, N. Ghori, H. G. Elmendorf, and W. L. Li.** 1991. The accumulation and metabolism of a fluorescent ceramide derivative in *Plasmodium falciparum*-infected erythrocytes. Mol. Biochem. Parasitol. **49:**143–156.
15. **Hawthorne, P. L., K. R. Trenholme, T. S. Skinner-Adams, T. Spielmann, K. Fischer, M. W. Dixon, M. R. Ortega, K. L. Anderson, D. J. Kemp, and D. L. Gardiner.** 2004. A novel *Plasmodium falciparum* ring stage protein, REX, is located in Maurer's clefts. Mol. Biochem. Parasitol. **136:**181–189.
16. **Hayashi, M., S. Taniguchi, Y. Ishizuka, H. S. Kim, Y. Wataya, A. Yamamoto, and Y. Moriyama.** 2001. A homologue of N-ethylmaleimide-sensitive factor in the malaria parasite *Plasmodium falciparum* is exported and localized in vesicular structures in the cytoplasm of infected erythrocytes in the brefeldin A-sensitive pathway. J. Biol. Chem. **276:**15249–15255.
17. **Hiller, N. L., S. Bhattacharjee, C. van Ooij, K. Liolios, T. Harrison, C. Lopez-Estrano, and K. Haldar.** 2004. A host-targeting signal in virulence proteins reveals a secretome in malarial infection. Science **306:**1934–1937.
18. **Kaviratne, M., S. M. Khan, W. Jarra, and P. R. Preiser.** 2002. Small variant STEVOR antigen is uniquely located within Maurer's clefts in *Plasmodium falciparum*-infected red blood cells. Eukaryot. Cell **1:**926–935.
19. **Klonis, N., M. Rug, I. Harper, M. Wickham, A. Cowman, and L. Tilley.** 2002. Fluorescence photobleaching analysis for the study of cellular dynamics. Eur. Biophys. J. **31:**36–51.
20. **Knuepfer, E., M. Rug, N. Klonis, L. Tilley, and A. F. Cowman.** 2005. Trafficking determinants for PfEMP3 export and assembly under the *Plasmodium falciparum*-infected red blood cell membrane. Mol. Microbiol. **58:**1039–1053.
21. **Knuepfer, E., M. Rug, N. Klonis, L. Tilley, and A. F. Cowman.** 2005. Trafficking of the major virulence factor to the surface of transfected *P. falciparum*-infected erythrocytes. Blood **105:**4078–4087.
22. **Kriek, N., L. Tilley, P. Horrocks, R. Pinches, B. C. Elford, D. J. Ferguson, K. Lingelbach, and C. I. Newbold.** 2003. Characterization of the pathway for transport of the cytoadherence-mediating protein, PfEMP1, to the host cell surface in malaria parasite-infected erythrocytes. Mol. Microbiol. **50:**1215–1227.
23. **Kyes, S., P. Horrocks, and C. Newbold.** 2001. Antigenic variation at the infected red cell surface in malaria. Annu. Rev. Microbiol. **55:**673–707.
24. **Lanzer, M., H. Wickert, G. Krohne, L. Vincensini, and C. Braun Breton.** 2006. Maurer's clefts: a novel multi-functional organelle in the cytoplasm of Plasmodium falciparum-infected erythrocytes. Int. J. Parasitol. **36:**23–36.
25. **Lopez-Estrano, C., S. Bhattacharjee, T. Harrison, and K. Haldar.** 2003. Cooperative domains define a unique host cell-targeting signal in *Plasmodium falciparum*-infected erythrocytes. Proc. Natl. Acad. Sci. USA **100:**12402–12407.
26. **Marti, M., R. T. Good, M. Rug, E. Knuepfer, and A. F. Cowman.** 2004. Targeting malaria virulence and remodeling proteins to the host erythrocyte. Science **306:**1930–1933.
27. **Nakai, K., and P. Horton.** 1999. PSORT: a program for detecting sorting signals in proteins and predicting their subcellular localization. Trends Biochem. Sci. **24:**34–36.
28. **Orci, L., M. Ravazzola, P. Meda, C. Holcomb, H. P. Moore, L. Hicke, and R. Schekman.** 1991. Mammalian Sec23p homologue is restricted to the endoplasmic reticulum transitional cytoplasm. Proc. Natl. Acad. Sci. USA **88:**8611–8615.
29. **Przyborski, J. M., S. K. Miller, J. M. Pfahler, P. P. Henrich, P. Rohrbach, B. S. Crabb, and M. Lanzer.** 2005. Trafficking of STEVOR to the Maurer's clefts in *Plasmodium falciparum*-infected erythrocytes. EMBO J. **24:**2306–2317.
30. **Przyborski, J. M., H. Wickert, G. Krohne, and M. Lanzer.** 2003. Maurer's clefts–a novel secretory organelle? Mol. Biochem. Parasitol. **132:**17–26.
31. **Rug, M., M. E. Wickham, M. Foley, A. Cowman, and L. Tilley.** 2004. Correct promoter control is needed for trafficking of the ring-infected erythrocyte

surface antigen to the host cytosol in transfected malaria parasites. Infect. Immun. **72:**6095–6105.
32. **Sam-Yellowe, T. Y., L. Florens, J. R. Johnson, T. Wang, J. A. Drazba, K. G. Le Roch, Y. Zhou, S. Batalov, D. J. Carucci, E. A. Winzeler, and J. R. Yates III.** 2004. A Plasmodium gene family encoding Maurer's cleft membrane proteins: structural properties and expression profiling. Genome Res. **14:** 1052–1059.
33. **Sherman, I. W., S. Eda, and E. Winograd.** 2003. Cytoadherence and sequestration in *Plasmodium falciparum*: defining the ties that bind. Microbes Infect. **5:**897–909.
34. **Snow, R. W., C. A. Guerra, A. M. Noor, H. Y. Myint, and S. I. Hay.** 2005. The global distribution of clinical episodes of *Plasmodium falciparum* malaria. Nature **434:**214–217.
35. **Spielmann, T., and H. P. Beck.** 2000. Analysis of stage-specific transcription in *Plasmodium falciparum* reveals a set of genes exclusively transcribed in ring stage parasites. Mol. Biochem. Parasitol. **111:**453–458.
36. **Spielmann, T., D. J. Fergusen, and H. P. Beck.** 2003. etramps, a new *Plasmodium falciparum* gene family coding for developmentally regulated and highly charged membrane proteins located at the parasite-host cell interface. Mol. Biol. Cell **14:**1529–1544.
37. **Spycher, C., N. Klonis, T. Spielmann, E. Kump, S. Steiger, L. Tilley, and H. P. Beck.** 2003. MAHRP-1, a novel *Plasmodium falciparum* histidine-rich protein, binds ferriprotoporphyrin IX and localizes to the Maurer's clefts. J. Biol. Chem. **278:**35373–35383.
38. **Taraschi, T. F., M. E. O'Donnell, S. Martinez, T. Schneider, D. Trelka, V. M. Fowler, L. Tilley, and Y. Moriyama.** 2003. Generation of an erythrocyte vesicle transport system by *Plasmodium falciparum* malaria parasites. Blood **102:**3420–3426.
39. **Vincensini, L., S. Richert, T. Blisnick, A. Van Dorsselaer, E. Leize-Wagner, T. Rabilloud, and C. Braun Breton.** 2005. Proteomic analysis identifies novel proteins of the Maurer's clefts, a secretory compartment delivering *Plasmodium falciparum* proteins to the surface of its host cell. Mol. Cell Proteomics **4:**582–593.
40. **von Heijne, G.** 1992. Membrane protein structure prediction. Hydrophobicity analysis and the positive-inside rule. J. Mol. Biol. **225:**487–494.
41. **Waller, R. F., M. B. Reed, A. F. Cowman, and G. I. McFadden.** 2000. Protein trafficking to the plastid of *Plasmodium falciparum* is via the secretory pathway. EMBO J. **19:**1794–1802.
42. **Waterkeyn, J. F., M. E. Wickham, K. Davern, B. M. Cooke, J. C. Reeder, J. G. Culvenor, R. F. Waller, and A. F. Cowman.** 2000. Targeted mutagenesis of *Plasmodium falciparum* erythrocyte membrane protein 3 (PfEMP3) disrupts cytoadherence of malaria-infected red blood cells. EMBO J. **19:**2813–2823.
43. **Wickert, H., W. Gottler, G. Krohne, and M. Lanzer.** 2004. Maurer's cleft organization in the cytoplasm of *Plasmodium falciparum*-infected erythrocytes: new insights from three-dimensional reconstruction of serial ultrathin sections. Eur. J. Cell Biol. **83:**567–582.
44. **Wickert, H., P. Rohrbach, S. J. Scherer, G. Krohne, and M. Lanzer.** 2003. A putative Sec23 homologue of *Plasmodium falciparum* is located in Maurer's clefts. Mol. Biochem. Parasitol. **129:**209–213.
45. **Wickert, H., F. Wissing, K. T. Andrews, A. Stich, G. Krohne, and M. Lanzer.** 2003. Evidence for trafficking of PfEMP1 to the surface of *P. falciparum*-infected erythrocytes via a complex membrane network. Eur. J. Cell Biol. **82:**271–284.
46. **Wickham, M. E., M. Rug, S. A. Ralph, N. Klonis, G. I. McFadden, L. Tilley, and A. F. Cowman.** 2001. Trafficking and assembly of the cytoadherence complex in *Plasmodium falciparum*-infected human erythrocytes. EMBO J. **20:**5636–5649.